HHS Public Access

Author manuscript

Dev Biol. Author manuscript; available in PMC 2017 October 15.

Published in final edited form as:

Dev Biol. 2016 October 15; 418(2): 242–247. doi:10.1016/j.ydbio.2016.08.029.

Knockdown of the pericellular matrix molecule perlecan lowers in situ cell and matrix stiffness in developing cartilage

Xin Xu[a,1], **Zhiyu Li**[b,1], **Yue Leng**[b], **Corey P. Neu**[a], and **Sarah Calve**[b,*]

Corey P. Neu: cpneu@colorado.edu; Sarah Calve: scalve@purdue.edu

[a]Department of Mechanical Engineering, University of Colorado Boulder, 1111 Engineering Drive, Boulder, CO 80309

[b]Weldon School of Biomedical Engineering, Purdue University, 206 South Martin Jischke Drive, West Lafayette, IN 47907

Abstract

The pericellular matrix (PCM) is a component of the extracellular matrix that is found immediately surrounding individual chondrocytes in developing and adult cartilage, and is rich in the proteoglycan perlecan. Mutations in perlecan are the basis of several developmental disorders, which are thought to arise from disruptions in the mechanical stability of the PCM. We tested the hypothesis that defects in PCM organization will reduce the stiffness of chondrocytes in developing cartilage by combining a murine model of Schwartz-Jampel syndrome, in which perlecan is knocked down, with our novel atomic force microscopy technique that can measure the stiffness of living cells and surrounding matrix in embryonic and postnatal tissues *in situ*. Perlecan knockdown altered matrix organization and significantly decreased the stiffness of both chondrocytes and interstitial matrix as a function of age and genotype. Our results demonstrate that the knockdown of a spatially restricted matrix molecule can have a profound influence on cell and tissue stiffness, implicating a role for outside-in mechanical signals from the PCM in regulating the intracellular mechanisms required for the overall development of cartilage.

Keywords

atomic force microscopy; mechanobiology; chondrocyte; pericellular matrix

[*]Corresponding Authors: Tel: +(765) 496 1768; fax: +(765) 494 0902.

[1]these authors contributed equivalently to this work

Competing interests

The authors declare no competing interests.

Author contributions

S.C. and C.P.N. conceived of the experiments. S.C., X.X., Z.L. and C.P.N. designed the experiments. X.X., Z.L. and Y.L. performed the experiments and analyzed and interpreted the data. S.C., X.X., Z.L. and C.P.N. wrote the manuscript. All authors critically reviewed the manuscript.

Introduction

The extracellular matrix (ECM) in mature cartilage of the limb has two distinct regions: A pericellular matrix (PCM) that tightly surrounds individual chondrocytes and an interstitial matrix that fills the space between chondrocytes. The interstitial matrix contains type II collagen fibrils to withstand tensile loads and space-filling aggrecan-hyaluronic acid complexes to provide resistance during compression (Han et al., 2011). The PCM of mature cartilage is predominantly composed of type VI collagen and perlecan and thought to simultaneously mediate the transduction of mechanical forces and protect the cells from cyclic mechanical loading (Guilak et al., 2006). Perlecan, encoded by the heparan sulfate proteoglycan-2 (*Hspg2*) gene, is present in all basement membranes and the PCM mature cartilage. Within developing cartilage, perlecan is deposited after the onset of mesenchymal condensation and becomes highly expressed in the growth plate (Costell et al., 1999). Perlecan sequesters many growth factors, including those from the fibroblast growth factor (FGF) family, which likely facilitate the ability of perlecan to potentiate chondrogenesis (French et al., 1999; Vincent et al., 2007). In addition, perlecan is also thought to contribute to the mechanical stability of tissues as it has been shown that in perlecan knockout mice, basement membranes degrade in regions of increased mechanical loading (Costell et al., 1999). Furthermore, the shape deformity of long bones in perlecan knockout mice is hypothesized to result from abnormal organization of the hypertrophic matrix that may have a lower resistance to mechanical forces generated by muscle contraction (Costell et al., 1999).

Mutations in perlecan have been shown to be the basis of several human disorders. Dissegmental dysplasia, Silverman-Handmaker type is a lethal autosomal recessive form of short-limbed dwarfism due to mutations that prevent perlecan secretion (Arikawa-Hirasawa et al., 2001). A non-lethal disorder linked to perlecan dysregulation is Schwartz-Jampel syndrome (SJS), which can be caused by a number of mutations that interfere with perlecan function but not its secretion, and is characterized by generalized muscle stiffness with chondrodysplasia (Nicole et al., 2000; Stum et al., 2008). These developmental disorders may arise due to the hypothesized role of perlecan in mechanically stabilizing the pericellular matrix (Costell et al., 1999).

The study of the mechanics of single cells embedded in their native matrix has largely been unexplored due to the difficulty in accessing and maintaining viable cells using conventional approaches and existing biophysical techniques. While the influence of the interstitial ECM on cartilage mechanics, e.g. aggrecan and type II collagen, has been extensively studied at the tissue scale (Buschmann et al., 1999; Darling et al., 2004; Sharma et al., 2013), only recently has attention been focused towards the biomechanical measurement of the PCM with the adoption of atomic force microscopy (AFM) as a testing modality (Alexopoulos et al., 2009; Wilusz et al., 2012). AFM is the primary methodology utilized to resolve differences in mechanical properties at the cellular level; however, the geometry and heterogeneity of most tissues precludes the testing of intact specimens. To circumvent this problem, sections of homogeneous thickness are obtained using a cryotome and have revealed significant differences in cartilage biomechanics (Alexopoulos et al., 2009; Klein et al., 2007; Mahmoodian et al., 2011; Prein et al., 2015; Tesche and Miosge, 2004;

Williamson et al., 2001; Wilusz et al., 2012). Unfortunately, freezing leads to cell death and prevents the direct measurement of cell mechanics within the native ECM. Furthermore, freezing of biological tissues can alter bulk ECM mechanics (Bischof and He, 2005; Venkatasubramanian et al., 2010), indicating measurements on cryosections likely do not reflect the true material properties.

To address the need to accurately measure the mechanics of heterogeneous tissues, we developed a technique that maintains cell viability while enabling the precise AFM study of chondrocytes and the surrounding matrix within a controlled culture system (Xu et al., 2016). Furthermore, we demonstrated significant differences in cryotomed vs. vibratomed sections, illustrating the ability to study viable cells and need to the avoid cryosectioning in order to prevent loss of native tissue properties (Xu et al., 2016). In this study, we used this tool to test the hypothesis that defects in PCM organization will reduce the stiffness of chondrocytes in developing cartilage. Using a murine model of SJS (Stum et al., 2008), we found that disruption of perlecan incorporation significantly decreases the stiffness of both the chondrocytes and the interstitial matrix during cartilage development.

Materials and Methods

Unless otherwise specified, all reagents were of chemical grade from Sigma-Aldrich

Embryo and pup harvest—Tissues from E16.5, E19.5 and P3 mice were generated by the timed mating of mice heterozygous for *Hspg2*$^{C1532Y\text{-}Neo}$ on a DBA background, kindly provided by Dr. Sophie Nicole (Inserm, France) (Stum et al., 2008). All murine experiments were approved by the Purdue Animal Care and Use Committee (PACUC; protocol 1310000973). Dams were euthanized via CO_2 inhalation, confirmed by cervical dislocation. Embryos were removed from the uterine horns and P3 mice were euthanized via decapitation. Forelimbs were removed from the body with microscissors and placed into ice-cold phosphate buffered saline (PBS) until processed for cryotome or vibratome sectioning. Tail snips were used to confirm genotypes as wild-type (+/+), heterozygous (Neo/+) or homozygous (Neo/Neo) for *Hspg2*$^{C1532Y\text{-}Neo}$ using the following primers (5′ → 3′) CCT CGA GGT GGA AGA GTG TC, GCT TGG CTC TTA GGG AGT GA, AAG GGG CCA CCA AAG AAC, which generated a 210 bp band for the wt and a 362 bp band for the mutant allele.

Processing of forelimbs for cryosectioning and immunohistochemistry—Before cryosectioning, forelimbs were embedded in Optimal Cutting Temperature compound (OCT, Sakura Finetek), frozen with dry ice-cooled isopentane and stored at -80°C until sectioned. 5 – 10μm cryosections were collected on His-bond^{+} glass slides (VWR) and washed with PBS for 3 times to remove any residual OCT before conducting AFM. Cryosections were processed following (Calve et al., 2010) and stained with primary antibodies against perlecan (1:50; Santa Cruz Biotechnology sc33707) and type VI collagen (1:200, Millipore AB7821) and then the secondary detection reagents [Alexa Fluor 647 anti-rabbit (1:500, Life Technologies), DyLight 550 anti-rat (1:250, Pierce), DAPI (1:500, Roche). Sections were imaged at 10x using a Leica DMI6000 inverted microscope and at 63x using a Zeiss 710 confocal microscope. Pictures were acquired using the same imaging

parameters across the different genotypes and processed under identical conditions using Adobe Photoshop.

Processing of forelimbs for cryosectioning and immunohistochemistry—For vibratome sectioning, the forelimbs were trimmed to remove the excess tissue away from the elbow to make the joint as small as possible while still keeping it intact. The joint was then immersed into tissue adhesive (Electron Microscopy Sciences) for about 3 seconds and then placed in 4% low gelling temperature agarose (Amresco) in PBS. Agarose-embedded samples were affixed to the sample holder of a Leica VT-1000S vibratome with Loctite and the chamber was filled with PBS to maintain sample hydration and viability. Forelimbs were sliced into 200 μm thick sections and were stored in Dulbecco's modified Eagle's medium (Life Technologies) on ice until analyzed the same day by AFM.

AFM analysis—Forelimb sections were mounted to glass coverslips using 0.5 μL tissue adhesive, making sure there was not any glue on the regions where AFM would be performed. A Keysight 5500 AFM system (Keysight Technologies) mounted on a Nikon Eclipse Ti wide-field inverted microscope (Nikon Instruments) was operated in force volume mode and the force trigger was set to approximately 11.5 nN indicating the point at which the cantilever approach was stopped and then retracted. By fitting the force-displacement curves to a Hertzian contact mechanics model, the compressive modulus was determined (Johnson et al., 1971), and a cantilever of known tip geometry was used (5 μm borosilicate glass sphere; NovaScan). The cantilever stiffness was pre-calibrated to be 0.07 N/m, by the thermal fluctuation method (Hutter and Bechhoefer, 1993). When the articular surface of the humerus was located, a very brief scan (4×4 grid) was performed to ensure the height change of the area was in the acceptable range (7 to 8 μm) of the cantilever. After that, a higher resolution scan was conducted to collect more detailed topography and stiffness maps (15μm×15μm or 30μm×30μm, 64×64 grid).

Statistical Analysis—Data for each time point were pooled from three independent litters in which all three genotypes were represented. Within each litter, one animal from each genotype was randomly selected for testing, and each animal was evaluated at $n \geq 3$ locations. For each location, a 5×5 pixel^2 matrix was taken from the AFM stiffness map at the middle of a cell and matrix region, to calculate average cell and ECM stiffness. The p-value was calculated using SPSS Statistics (IBM).

Results and Discussion

The organization of the PCM is disrupted in a murine model of SJS

To visualize how perlecan knockdown influences the architecture of developing cartilage, we utilized a model of SJS developed by the Nicole laboratory in which a c.4595 G to A point mutation in the perlecan gene (*Hspg2*) interferes with the incorporation of this ECM into the PCM network. Mice in which the neomyosin selection cassette was retained, $Hspg2^{C1532Y\text{-}Neo}$, have reduced perlecan secretion and display defects consistent with the clinical manifestations of human SJS (Rodgers et al., 2007; Stum et al., 2008). Specifically, mice homozygous for $Hspg2^{C1532Y\text{-}Neo}$ (Neo/Neo) have short stature, impaired

mineralization, misshapen bones, OA-like joint dysplasias and myotonia (Rodgers et al., 2007; Stum et al., 2008).

Cryosections of the developing humerus from wild type (+/+), heterozygous (Neo/+) and homozygous (Neo/Neo) mice at embryonic day (E)16.5 and postnatal day (P)3 were stained for perlecan (red) and type VI collagen (green; Fig. 1). Homozygous animals showed low levels of perlecan that appeared to be restricted to the intracellular compartment, which is consistent with a previous report that showed that perlecan in (Neo/Neo) mice is sequestered in the endoplasmic reticulum and is likely degraded (Lowe et al., 2014). In heterozygous and wild-type E16.5 embryos, perlecan was found throughout the distal humerus, (Fig. 1 B – C′), similar to what has been shown in the elbow of the developing human (Hayes et al., 2016). By P3, perlecan and type VI collagen became more restricted to the pericellular matrix in heterozygous and wild-type animals as the cells became more spread out (Fig. 1E – F′). Type VI collagen reactivity was reduced in homozygous animals and was relatively disorganized in the center of the tissue (*, D), which can be attributed to the disruption of perlecan – type VI collagen binding (Tillet et al., 1994).

Measurement of the *In Situ* Biomechanical Properties of Viable Developing Cartilage

The mechanical properties of prenatal cartilage has been previously characterized (Klein et al., 2007; Mahmoodian et al., 2011; Prein et al., 2015; Williamson et al., 2001); however, these studies were not able to distinguish between cell and matrix stiffness due to either the use of cryotomed sections or the testing modality. To directly investigate cell and ECM mechanics in developing cartilage, 200 μm thick sections of fresh embryonic and neonatal murine forelimbs were generated with a vibratome (Fig. 2*A*). Sections containing the articular surface of the distal humerus were affixed to a glass coverslip using tissue adhesive then placed in a PBS-filled liquid cell to acquire stiffness maps via AFM (Fig. 2B). Cells within the developing forelimb remained viable over the day of testing as indicated by using a live (green) – dead (red) cell assay (70 – 90% viability; Fig. 2B). Stiffness of the tissue was then measured using AFM (Fig. 2C). For our initial experiments, vibratome sections were stained for type VI collagen after AFM analysis and aligned with stiffness maps to assist in differentiating between cell and ECM compressive moduli (Fig. 2D). Plotting the stiffness map from Fig. 2C in 3D as a function of height revealed our measurements were not influenced by variations in topography (Fig. 2D).

Representative force – displacement curves reveal the increased compliance and lower stiffness of cryotomed vs. vibratomed cartilage (Fig. 2E). We previously demonstrated, freezing significantly lowers cell and ECM stiffness (Xu et al., 2016). One reason for the significant difference in stiffness may be from the freezing process disrupting interactions between cells and microenvironment since the live cells can hold the matrices together and maintain tissue integrity, whereas the dead cells can no longer maintain tension on the surrounding matrix and potentially also release enzymes that influence the structure and components of the matrices.

Perlecan knock-down significantly decreases cell and ECM stiffness in developing cartilage

To directly test how alterations in matrix composition affect the stiffness of developing cartilage, we analyzed vibratome sections of wild type (+/+), heterozygous (Neo/+) and homozygous (Neo/Neo) mice with AFM. Care was taken to analyze the distal-most regions of the developing humerus, as this area would remain cartilaginous upon maturation (box, Fig. 2B). High-resolution AFM stiffness maps show an increase in stiffness as a function of age and perlecan incorporation for both ECM and cells (Fig. 3A). Sections of each map were subdivided into 5 × 5 px regions representative of cells or ECM to determine how perlecan knockdown affected different components of the tissue. Two-way ANOVA analysis of ECM and cell stiffness reveals a significant effect of age ($p<0.0001$) and genotype ($p<0.0001$; Fig. 3B), and the interaction between age and genotype was significant for both components ($p<0.01$).

The increase in ECM compressive modulus from E16.5 to P3 in wild type animals reflects the transition from a perlecan-rich developmental matrix to a more mature aggrecan-rich ECM (Melrose et al., 2005). While the cells are significantly less stiff than the matrix, the corresponding increase in stiffness with age, as well as the decrease due to perlecan knockdown, is consistent with published observations that cell modulus is influenced by the external environment (Solon et al., 2007). Indeed, we previously demonstrated using the same AFM-based method that enzymatic disruption of hyaluronic acid in the ECM of adult bovine cartilage increased the stiffness of both the matrix and cells (Xu et al., 2016). The variations we observed in the compressive modulus of the bulk ECM may be indirectly related to the ability of perlecan to bind with various components of the matrix (Farach-Carson et al., 2014). In the context of cartilage, perlecan has been shown to play a role in the assembly of type II collagen fibrils (Gustafsson et al., 2003; Kvist et al., 2006). In addition, fibrillin-1 microfibrils, which occur as part of the elastin and microfibrillar networks in cartilage (Yu and Urban, 2010), connect with perlecan in the basement membrane and are disrupted in the intervertebral disc in the *hspg2*Δ^{3-}/Δ^{3-} exon 3 null mouse (Hayes et al., 2013; Tiedemann et al., 2005). Disruption of these components likely alters the overall structure of the interstitial matrix since it was shown that aggrecan was disorganized in the cartilage of (Neo/Neo) neonates (Lowe et al., 2014), which accounts for our observation that overall ECM stiffness decreases as a result of perlecan knockdown (Fig. 3). Perlecan knockdown also results in reduced skeletal muscle strength due to alterations in the neuromuscular junction (Stum et al., 2008), which has the potential to affect embryonic motility. Since many studies have demonstrated the requirement of mechanical loading for proper musculoskeletal development (Shea et al., 2015), a decrease of intrauterine movement in (Neo/Neo) and (Neo/+) mice may also have contributed to a decrease in ECM compressive modulus.

Another reason for the decrease in stiffness may be due to altered ECM deposition from disrupted signaling since perlecan binds many growth factors, including FGF-2 and -18 (Farach-Carson et al., 2014; Melrose et al., 2008). It is thought that perlecan acts as a sink for FGF-2 to keep it inactive until released due to PCM disruption (Vincent et al., 2007); however, the precise influence on FGF-2 on matrix metabolism remains unclear (Ellman et

al., 2013). FGF-18 is also expressed in the developing cartilage (Liu et al., 2002; Ohbayashi et al., 2002), and has been shown to have a positive effect on ECM anabolism by inducing the production of type II collagen and proteoglycans (Ellsworth et al., 2002). These two examples indicate that the decrease in bulk matrix stiffness in mice carrying the *Hspg2*$^{C1532Y\text{-}Neo}$ gene was likely indirectly influenced by disrupted growth factor signaling in addition to the direct effect of perlecan on ECM organization.

In order to separate out the biochemical and mechanical roles, it will be necessary to generate point mutations that disrupt growth factor binding but not the mechanical stability of perlecan. Once this has been achieved, our data will provide a baseline for these future studies. Nonetheless, our results indicate that perlecan knockdown alters matrix organization and stiffness, and additionally cell stiffness, which suggests that the physical cues required for the healthy development of cartilage are negatively impacted.

Acknowledgments

The authors would like to thank Dr. Edward Bartlett for use of his vibratome and the Purdue University Life Science Imaging Center.

Funding

This work was supported by the National Institutes of Health [R03 AR065201 to S.C.; R01 AR063712 and R21 AR066230 to C.P.N.] and the National Science Foundation [CMMI 1100554 to C.P.N.].

References

Alexopoulos LG, Youn I, Bonaldo P, Guilak F. Developmental and osteoarthritic changes in Col6a1-knockout mice: biomechanics of type VI collagen in the cartilage pericellular matrix. Arthritis Rheum. 2009; 60:771–779. [PubMed: 19248115]

Arikawa-Hirasawa E, Wilcox WR, Le AH, Silverman N, Govindraj P, Hassell JR, Yamada Y. Dyssegmental dysplasia, Silverman-Handmaker type, is caused by functional null mutations of the perlecan gene. Nat Genet. 2001; 27:431–434. [PubMed: 11279527]

Bischof JC, He X. Thermal stability of proteins. Ann NY Acad Sci. 2005; 1066:12–33. [PubMed: 16533916]

Buschmann MD, Kim YJ, Wong M, Frank E, Hunziker EB, Grodzinsky AJ. Stimulation of aggrecan synthesis in cartilage explants by cyclic loading is localized to regions of high interstitial fluid flow. Arch Biochem Biophys. 1999; 366:1–7. [PubMed: 10334856]

Calve S, Odelberg SJ, Simon HG. A transitional extracellular matrix instructs cell behavior during muscle regeneration. Dev Biol. 2010; 344:259–271. [PubMed: 20478295]

Costell M, Gustafsson E, Aszodi A, Morgelin M, Bloch W, Hunziker E, Addicks K, Timpl R, Fassler R. Perlecan maintains the integrity of cartilage and some basement membranes. J Cell Biol. 1999; 147:1109–1122. [PubMed: 10579729]

Darling EM, Hu JC, Athanasiou KA. Zonal and topographical differences in articular cartilage gene expression. J Orthop Res. 2004; 22:1182–1187. [PubMed: 15475195]

Ellman MB, Yan D, Ahmadinia K, Chen D, An HS, Im HJ. Fibroblast growth factor control of cartilage homeostasis. J Cell Biochem. 2013; 114:735–742. [PubMed: 23060229]

Ellsworth JL, Berry J, Bukowski T, Claus J, Feldhaus A, Holderman S, Holdren MS, Lum KD, Moore EE, Raymond F, Ren H, Shea P, Sprecher C, Storey H, Thompson DL, Waggie K, Yao L, Fernandes RJ, Eyre DR, Hughes SD. Fibroblast growth factor-18 is a trophic factor for mature chondrocytes and their progenitors. Osteoarthr Cartilage. 2002; 10:308–320.

Farach-Carson MC, Warren CR, Harrington DA, Carson DD. Border patrol: insights into the unique role of perlecan/heparan sulfate proteoglycan 2 at cell and tissue borders. Matrix Biol. 2014; 34:64–79. [PubMed: 24001398]

French MM, Smith SE, Akanbi K, Sanford T, Hecht J, Farach-Carson MC, Carson DD. Expression of the heparan sulfate proteoglycan, perlecan, during mouse embryogenesis and perlecan chondrogenic activity in vitro. J Cell Biol. 1999; 145:1103–1115. [PubMed: 10352025]

Guilak F, Alexopoulos LG, Upton ML, Youn I, Choi JB, Cao L, Setton LA, Haider MA. The pericellular matrix as a transducer of biomechanical and biochemical signals in articular cartilage. Ann N Y Acad Sci. 2006; 1068:498–512. [PubMed: 16831947]

Gustafsson E, Aszodi A, Ortega N, Hunziker EB, Denker HW, Werb Z, Fassler R. Role of collagen type II and perlecan in skeletal development. Ann N Y Acad Sci. 2003; 995:140–150. [PubMed: 12814946]

Han L, Grodzinsky AJ, Ortiz C. Nanomechanics of the Cartilage Extracellular Matrix. Ann Rev Mater Res. 2011; 41:133–168. [PubMed: 22792042]

Hayes AJ, Hughes CE, Smith SM, Caterson B, Little CB, Melrose J. The CS Sulfation Motifs 4C3, 7D4, 3B3[−]; and Perlecan Identify Stem Cell Populations and Their Niches, Activated Progenitor Cells and Transitional Areas of Tissue Development in the Fetal Human Elbow. Stem Cells Dev. 2016; 25:836–847. [PubMed: 27068010]

Hayes AJ, Smith SM, Melrose J. Comparative immunolocalisation of fibrillin-1 and perlecan in the human foetal, and HS-deficient hspg2 exon 3 null mutant mouse intervertebral disc. Histochem Cell Biol. 2013; 139:1–11. [PubMed: 23104139]

Hutter JL, Bechhoefer J. Calibration of atomic-force microscope tips. Rev Sci Instrum. 1993; 64:1868–1873.

Johnson KL, Kendall K, Roberts AD. Surface energy and contact of elastic solids. P Roy Soc A - Math Phys. 1971; 324:301–313.

Klein TJ, Chaudhry M, Bae WC, Sah RL. Depth-dependent biomechanical and biochemical properties of fetal, newborn, and tissue-engineered articular cartilage. J Biomech. 2007; 40:182–190. [PubMed: 16387310]

Kvist AJ, Johnson AE, Morgelin M, Gustafsson E, Bengtsson E, Lindblom K, Aszodi A, Fassler R, Sasaki T, Timpl R, Aspberg A. Chondroitin sulfate perlecan enhances collagen fibril formation. Implications for perlecan chondrodysplasias. J Biol Chem. 2006; 281:33127–33139. [PubMed: 16956876]

Liu Z, Xu J, Colvin JS, Ornitz DM. Coordination of chondrogenesis and osteogenesis by fibroblast growth factor 18. Genes Dev. 2002; 16:859–869. [PubMed: 11937493]

Lowe DA, Lepori-Bui N, Fomin PV, Sloofman LG, Zhou X, Farach-Carson MC, Wang L, Kirn-Safran CB. Deficiency in perlecan/HSPG2 during bone development enhances osteogenesis and decreases quality of adult bone in mice. Calcif Tissue Int. 2014; 95:29–38. [PubMed: 24798737]

Mahmoodian R, Leasure J, Philip P, Pleshko N, Capaldi F, Siegler S. Changes in mechanics and composition of human talar cartilage anlagen during fetal development. Osteoarthr Cartilage. 2011; 19:1199–1209.

Melrose J, Hayes AJ, Whitelock JM, Little CB. Perlecan, the “jack of all trades” proteoglycan of cartilaginous weight-bearing connective tissues. BioEssays. 2008; 30:457–469. [PubMed: 18404701]

Melrose J, Smith S, Cake M, Read R, Whitelock J. Perlecan displays variable spatial and temporal immunolocalisation patterns in the articular and growth plate cartilages of the ovine stifle joint. Histochem Cell Biol. 2005; 123:561–571. [PubMed: 16021525]

Nicole S, Davoine CS, Topaloglu H, Cattolico L, Barral D, Beighton P, Hamida CB, Hammouda H, Cruaud C, White PS, Samson D, Urtizberea JA, Lehmann-Horn F, Weissenbach J, Hentati F, Fontaine B. Perlecan, the major proteoglycan of basement membranes, is altered in patients with Schwartz-Jampel syndrome (chondrodystrophic myotonia). Nat Genet. 2000; 26:480–483. [PubMed: 11101850]

Ohbayashi N, Shibayama M, Kurotaki Y, Imanishi M, Fujimori T, Itoh N, Takada S. FGF18 is required for normal cell proliferation and differentiation during osteogenesis and chondrogenesis. Genes Dev. 2002; 16:870–879. [PubMed: 11937494]

Prein C, Warmbold N, Farkas Z, Schieker M, Aszodi A, Clausen-Schaumann H. Structural and mechanical properties of the proliferative zone of the developing murine growth plate cartilage assessed by atomic force microscopy. Matrix Biol. 2015

Rodgers KD, Sasaki T, Aszodi A, Jacenko O. Reduced perlecan in mice results in chondrodysplasia resembling Schwartz-Jampel syndrome. Hum Mol Genet. 2007; 16:515–528. [PubMed: 17213231]

Sharma S, Panitch A, Neu CP. Incorporation of an aggrecan mimic prevents proteolytic degradation of anisotropic cartilage analogs. Acta Biomater. 2013; 9:4618–4625. [PubMed: 22939923]

Shea CA, Rolfe RA, Murphy P. The importance of foetal movement for co-ordinated cartilage and bone development in utero: clinical consequences and potential for therapy. Bone Joint Res. 2015; 4:105–116. [PubMed: 26142413]

Solon J, Levental I, Sengupta K, Georges PC, Janmey PA. Fibroblast adaptation and stiffness matching to soft elastic substrates. Biophys J. 2007; 93:4453–4461. [PubMed: 18045965]

Stum M, Girard E, Bangratz M, Bernard V, Herbin M, Vignaud A, Ferry A, Davoine CS, Echaniz-Laguna A, Rene F, Marcel C, Molgo J, Fontaine B, Krejci E, Nicole S. Evidence of a dosage effect and a physiological endplate acetylcholinesterase deficiency in the first mouse models mimicking Schwartz-Jampel syndrome neuromyotonia. Hum Mol Genet. 2008; 17:3166–3179. [PubMed: 18647752]

Tesche F, Miosge N. Perlecan in late stages of osteoarthritis of the human knee joint. Osteoarthr Cartilage. 2004; 12:852–862.

Tiedemann K, Sasaki T, Gustafsson E, Gohring W, Batge B, Notbohm H, Timpl R, Wedel T, Schlotzer-Schrehardt U, Reinhardt DP. Microfibrils at basement membrane zones interact with perlecan via fibrillin-1. J Biol Chem. 2005; 280:11404–11412. [PubMed: 15657057]

Tillet E, Wiedemann H, Golbik R, Pan TC, Zhang RZ, Mann K, Chu ML, Timpl R. Recombinant expression and structural and binding properties of alpha 1(VI) and alpha 2(VI) chains of human collagen type VI. Eur J Biochem. 1994; 221:177–185. [PubMed: 8168508]

Venkatasubramanian RT, Wolkers WF, Shenoi MM, Barocas VH, Lafontaine D, Soule CL, Iaizzo PA, Bischof JC. Freeze-thaw induced biomechanical changes in arteries: role of collagen matrix and smooth muscle cells. Ann Biomed Eng. 2010; 38:694–706. [PubMed: 20108044]

Vincent TL, McLean CJ, Full LE, Peston D, Saklatvala J. FGF-2 is bound to perlecan in the pericellular matrix of articular cartilage, where it acts as a chondrocyte mechanotransducer. Osteoarthr Cartilage. 2007; 15:752–763.

Williamson AK, Chen AC, Sah RL. Compressive properties and function-composition relationships of developing bovine articular cartilage. J Orthop Res. 2001; 19:1113–1121. [PubMed: 11781013]

Wilusz RE, DeFrate LE, Guilak F. A biomechanical role for perlecan in the pericellular matrix of articular cartilage. Matrix Biol. 2012; 31:320–327. [PubMed: 22659389]

Xu X, Li Z, Cai L, Calve S, Neu CP. Mapping the Nonreciprocal Micromechanics of Individual Cells and the Surrounding Matrix Within Living Tissues. Sci Rep. 2016; 6:24272. [PubMed: 27067516]

Yu J, Urban JP. The elastic network of articular cartilage: an immunohistochemical study of elastin fibres and microfibrils. J Anat. 2010; 216:533–541. [PubMed: 20148992]

Highlights

- Perlecan and cartilage ECM is disrupted in murine model of Schwartz-Jampel Syndrome
- Stiffness of cells and surrounding ECM in E16.5 – P3 cartilage was measured via AFM
- Perlecan knockdown significantly decreased cell and ECM stiffness at all timepoints

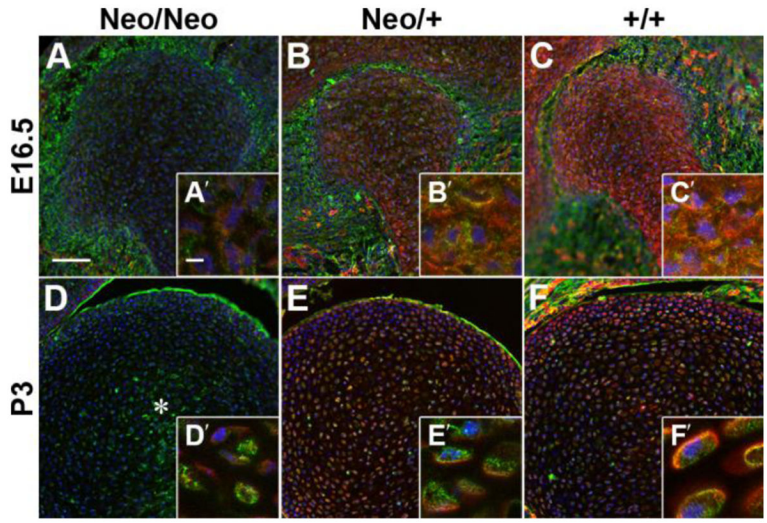

Figure 1. The chondrocyte PCM in the developing humerus is disrupted by perlecan knockdown

Cryosections from mice homozygous (A, D), heterozygous (B, E) or wild-type (C, F) for the mutation in *Hspg2* were stained for PCM components perlecan (red) and type VI collagen (green). Homozygous animals showed low levels of perlecan that appeared to be restricted to the intracellular compartment (A′, D′). In heterozygous and wild-type E16.5 embryos, perlecan was found throughout the developing cartilage, (B – C′). By P3, cell density decreased and perlecan became more restricted to the PCM in heterozygous and wild-type animals (E – F′). Type VI collagen reactivity was reduced in homozygous animals and was relatively disorganized in the center of the tissue (*, D). Blue = nuclei; bars: A = 75μm; A′ = 5μm.

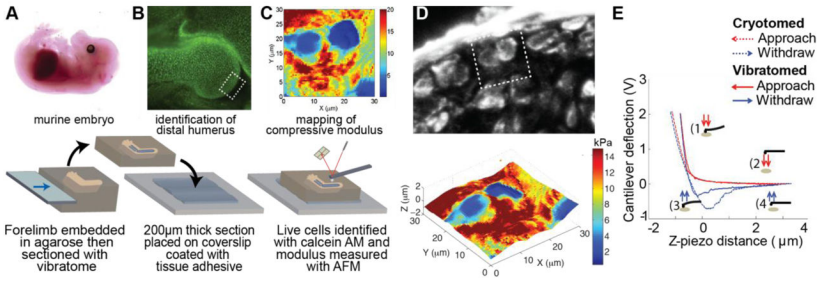

Fig. 2.

AFM on vibratome sections enables the study of the biomechanics of viable cells and the surrounding ECM.

(A) Forelimbs from freshly harvested murine embryos and pups were vibratomed to 200 μm thick. (B) All stiffness measurements were obtained proximal to the developing articular surface of the humerus (boxed region). Calcein-AM staining reveals cell viability is maintained throughout the forelimb. (C) Compressive modulus was measured the day of harvest via AFM. (D) Comparison of type VI collagen distribution and a surface height-stiffness map of the section shown in C (boxed region) indicates that stiffness of vibratomed samples is not dependent upon local topography. E) Representative force - displacement curves demonstrate that the stiffness of developing cartilage is dependent on whether the sections are vibratomed or cryotomed, see also (Xu et al., 2016).

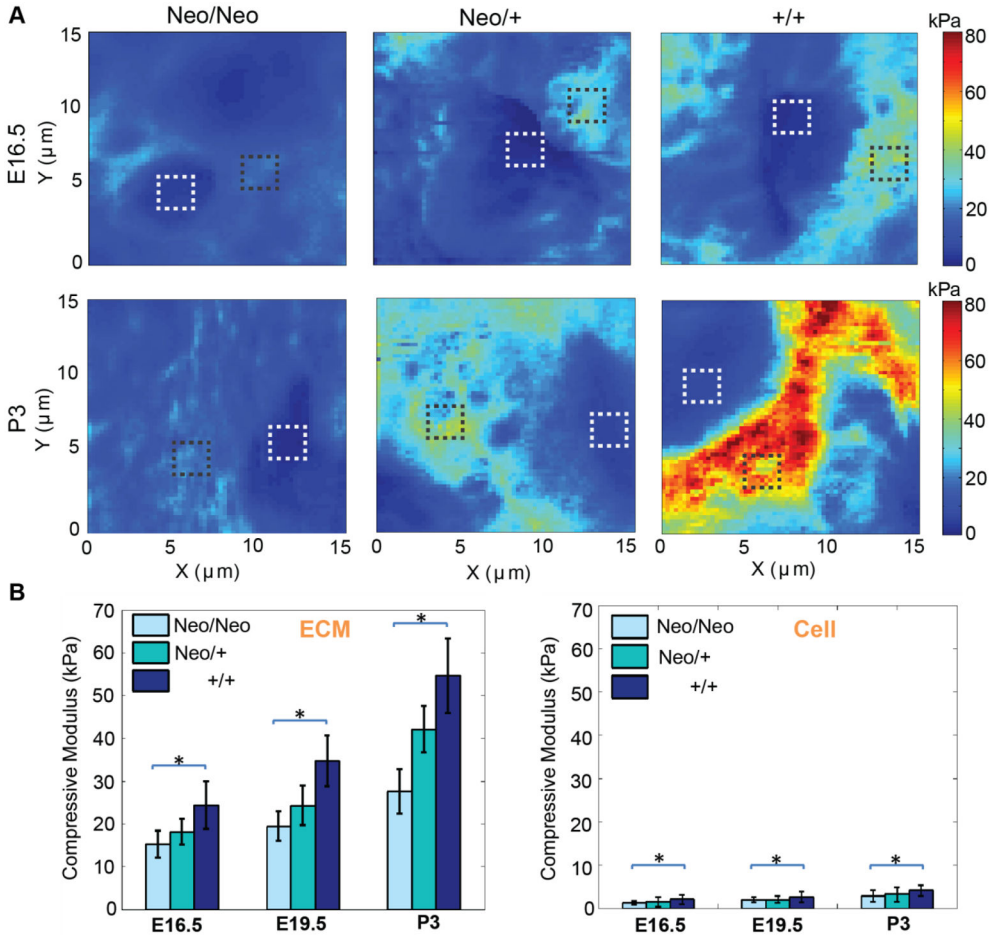

Figure 3. Perlecan knockdown significantly decreases the stiffness of the cells and ECM in developing articular cartilage

A) High-resolution stiffness maps show an increase in stiffness with age and perlecan incorporation. Boxes indicate representative regions where cell (white) and ECM (black) stiffness were measured. B) Both cell and ECM stiffness are influenced by perlecan content (*p<0.0001). Two-way ANOVA analysis of ECM and cell stiffness reveals a significant effect of age (p<0.0001) and genotype (p<0.0001). The interaction between age and genotype was significant for both components of the tissue (p<0.01). Data for each time point were pooled from three independent litters in which all three genotypes were represented. Error bars = s.d.